

Published in final edited form as:

Chembiochem. 2010 January 4; 11(1): 59–62. doi:10.1002/cbic.200900597.

A Prochelator Activated by Hydrogen Peroxide Prevents Metal-Induced Amyloid Beta Aggregation

Marina G. Dickens^a and Katherine J. Franz^a

Katherine J. Franz: katherine.franz@duke.edu

^a Department of Chemistry, Duke University, P.O. Box 90346 Durham, NC 27708, Fax: (+1-919-660-1605)

Keywords

Alzheimer's disease; amyloid; bioinorganic chemistry; copper; hydrogen peroxide

Alzheimer's is a progressive and fatal brain disease that is the most common form of dementia. Its characteristic pathology includes extracellular amyloid plaques that form as a result of abnormal clearance and/or increased production of amyloid- β peptides ($A\beta$) that are released from the amyloid precursor protein (APP).[1,2] Metal ions, particularly Cu^{+2+} and Zn^{2+} but also $Fe^{2+/3+}$, have been implicated in two processes related to $A\beta$ pathology: peptide aggregation and formation of reactive oxygen species (ROS).[3]

It is speculated that both APP and $A\beta$ may have normal roles in copper homeostasis.[4,5] It has also been shown in vitro that $A\beta$ can act as an antioxidant by quenching free radicals and/or by chelating copper.[6,7] Other evidence, however, suggests that $A\beta$ -Cu complexes are pro-oxidant and directly culpable of neurotoxicity.[8] In vitro, $A\beta$ in the presence of copper or iron and reducing agents like ascorbate produces H_2O_2 ,[9–11] which can subsequently react with the reduced metal ions to produce OH^\bullet via the Fenton reaction (Eq. 1).[12,13] Metal-mediated H_2O_2 generation appears at an early stage during in vitro $A\beta$ aggregation,[10,11] which supports the notion that soluble $A\beta$ -Cu species are responsible for the oxidative damage that is one of the earliest pathological events in Alzheimer's disease.[14] Furthermore, copper has been shown to intensify $A\beta$ toxicity in primary cortical neurons.[9,10,15] Like Cu^{2+} , Zn^{2+} also promotes $A\beta$ aggregation in vitro, but the Zn-induced aggregates may be neuroprotective. [16–18]



One hypothesis to reconcile the seemingly contradictory evidence related to metals, $A\beta$, and oxidative stress is that metal binding and $A\beta$ aggregation may represent an initial, protective response to dampen production of ROS. Excessive H_2O_2 and an overburden of copper could eventually push the system into a vicious cycle that switches $A\beta$ -Cu activity from antioxidant to pro-oxidant.[19] During this stage, metal exchange with Zn^{2+} could promote further $A\beta$ aggregation as a defense against copper-induced damage. While chelating agents are known

Correspondence to: Katherine J. Franz, katherine.franz@duke.edu.

Supporting information for this article is available on the WWW under <http://www.chembiochem.org>.

to reverse metal-induced aggregates, this model suggests that disaggregating plaques alone could have the unintended consequence of exacerbating oxidative damage. [19]

Metal chelating agents have appeared as a compelling strategy for Alzheimer's therapies. [20] In particular, 8-hydroxyquinoline (8HQ) derivatives clioquinol and PBT2 have shown promising results in mouse models and phase IIa clinical trials of Alzheimer's patients.[21, 22] These compounds inhibit metal-induced A β aggregation and ROS generation. While these reports encourage further development of metal-targeted compounds for neurodegenerative disease, there remain significant concerns about manipulating metal distribution in the brain. [23,24] Given the complexity of the metallobiology in Alzheimer's, it is particularly challenging to design metal-binding agents that can mitigate the damaging effects of metals while preserving their beneficial properties. In our lab, we are developing prochelators that are designed to bind metals only under conditions of oxidative stress.[25–27] The indications that elevated production of H₂O₂ by deviant Cu-A β interactions may trigger neurodegeneration suggested to us that prochelators activatable by H₂O₂ may be beneficial for managing a metal burden at locations of disease progression without stimulating widespread metal redistribution. Here, we present a boronic ester-masked 8-hydroxyquinoline derivative called **QBP** that converts to 8HQ in the presence of H₂O₂. Once converted to 8HQ, it is available for coordinating metal ions, as shown in Scheme 1 for Cu²⁺. The protecting group is ultimately released as pinanediol and non-toxic boric acid.[28,29]

QBP was synthesized by reacting commercially available quinoline boronic acid (QBA) with pinanediol in a Dean Stark apparatus. The X-ray crystal structure is shown in Figure 1. QBP is stable in aqueous solution between pH 5–8 over the course of 10 h, although some hydrolysis to QBA occurs at lower and higher pH values, as monitored by UV-Vis and mass spectrometry (data not shown).

With the phenol of 8HQ masked by the pinanediol boronic ester, the QBP prochelator should have little to no affinity for metal ions. A comparison of the UV-vis spectra in Figure 2 of QBP alone or in the presence of Cu²⁺ for an hour reveals no change in spectral features and validates the assumption that QBP does not interact with Cu²⁺ in its prochelator form. Addition of H₂O₂, however, causes a new spectrum to appear that matches that of [Cu(8HQ)₂], consistent with the reaction in Scheme 1.

In order to determine the rate of conversion of QBP to 8HQ by H₂O₂, reactions were monitored spectrophotometrically under pseudo first-order conditions of excess H₂O₂. The observed rate constants (k_{obs}) were plotted against peroxide concentration to give a rate constant k of 0.25 M⁻¹s⁻¹ (see the Supporting Information).

Chelators, including those based on the 8HQ motif, have been shown to have a dramatic effect on metal-induced A β aggregation.[30] Here, we monitored the metal-induced aggregation of A β by two complementary methods: light scattering, which reports the change in solution turbidity as a result of precipitate formation, and soluble protein concentration, which ascertains the fraction of protein that did not precipitate from solution. These methods provide a preliminary assessment of aggregation propensity, but do not report on detailed morphological changes of aggregates or fibrils.[31] In the light scattering assay, turbidity is assessed as the difference in absorbance at 405 nm between the sample and its matched control that contains the same components but without A β . The black, left-hand bars in Figure 3 show that, as previously observed by others,[32,33] both Cu²⁺ and Zn²⁺ increase the turbidity of A β samples, with Zn²⁺ causing a more profound effect. The presence of 2 equiv of 8HQ inhibits the Cu²⁺-induced aggregation and significantly reduces Zn²⁺-induced aggregation. After an hour of incubation, the aggregated peptide was removed by centrifugation and the amount of soluble peptide remaining was determined by a BCA assay. The gray, right-hand bars in Figure

3 show that samples treated with Cu^{2+} alone have only 60% soluble peptide, while those containing 8HQ have greater than 90% soluble $\text{A}\beta$. Similar results are seen for Zn^{2+} , with greater than 80% of the peptide remaining soluble when 8HQ is present. These data corroborate the turbidity assay and show that 8HQ present at the outset of metal- $\text{A}\beta$ incubations prevents aggregation. If 8HQ is added to pre-formed metal- $\text{A}\beta$ aggregates, the turbidity of the solutions decreases (see Supp. Info.), demonstrating that 8HQ can both prevent and reverse $\text{A}\beta$ aggregation under these conditions.

QBP, on the other hand, does not interfere with metal-induced $\text{A}\beta$ aggregation. The black, left-hand bars of Figure 4 show that the presence of QBP does not change the turbidity of solutions containing $\text{A}\beta$ alone or $\text{A}\beta$ plus Cu^{2+} . These results show that QBP itself neither induces nor prevents metal-induced $\text{A}\beta$ aggregation, as predicted based on its lack of metal-binding ability.

In order to show that the 8HQ that is generated in situ from the reaction of QBP and H_2O_2 is capable of reversing $\text{A}\beta$ aggregation, 1 mM H_2O_2 was added to each of the samples in Figure 4 that already contained Cu^{2+} -aggregated $\text{A}\beta$. The gray bars in Figure 4 show that H_2O_2 alone does not reduce the turbidity of samples containing $\text{A}\beta$ and Cu^{2+} , nor does it increase the turbidity of samples containing $\text{A}\beta$ alone or $\text{A}\beta/\text{Cu}^{2+}/8\text{HQ}$. These results show that H_2O_2 itself does not influence the aggregation state of $\text{A}\beta$. In contrast, samples that contain $\text{A}\beta/\text{Cu}^{2+}/\text{QBP}$ show a significant decrease in turbidity 30 min following H_2O_2 addition. This result is consistent with conversion of QBP to 8HQ, which can subsequently bind Cu^{2+} and reverse $\text{A}\beta$ aggregation. Given the concentrations of QBP and H_2O_2 present in the samples and the rate constant for prochelator-to-chelator conversion, this reaction is predicted to generate 9–45 μM 8HQ, depending on the initial QBP concentration. The highest concentration is certainly sufficient for complete binding of Cu^{2+} in a 1:2 complex, although as shown in the Figure, even the lower concentration is effective.

Confirmation that $[\text{Cu}(8\text{HQ})_2]$ is generated in the reaction of $\text{A}\beta/\text{Cu}/\text{QBP}/\text{H}_2\text{O}_2$ described in Figure 4 comes from mass spectral detection of 352 m/z , which is consistent with $[\text{Cu}(8\text{HQ})_2]$. Further evidence comes from the UV-vis spectrum of the reaction mixture, shown in Figure 5. The complex $[\text{Cu}(8\text{HQ})_2]$ has a characteristic absorbance band at 375 nm, which is clearly visible in samples that contain $\text{A}\beta$, Cu^{2+} and 8HQ. Samples that contain $\text{A}\beta/\text{Cu}/\text{QBP}/\text{H}_2\text{O}_2$ also show this characteristic peak, verifying that $[\text{Cu}(8\text{HQ})_2]$ has indeed been generated. This absorbance band tails into the 405 nm region used for monitoring turbidity, but its contribution was appropriately accounted for by subtracting the matched control from the sample value, ensuring that residual A_{405} reported in Figures 3 and 4 can be attributed to turbidity.

The previous experiment contained a relatively high concentration (1 mM) of H_2O_2 that was added in a single bolus. Several groups have shown that combinations of $\text{A}\beta$, Cu^{2+} and reductants produce significant amounts of H_2O_2 from O_2 . [10,34] Therefore, to investigate whether these conditions of more biologically relevant H_2O_2 production are sufficient for activating QBP, samples of $\text{A}\beta$, Cu^{2+} , ascorbic acid, and either 8HQ or QBP were monitored for H_2O_2 production with the Amplex Red/horseradish peroxidase (HRP) assay. Figure 6 shows the concentration of H_2O_2 detected by Amplex Red after a 1-h incubation of 200 nM $\text{Cu}(\text{Gly})_2$, 200 nM $\text{A}\beta$, 10 μM ascorbic acid and either 8HQ or QBP over a range of concentrations in sodium phosphate buffer at pH 7.4. Samples that contain Cu^{2+} and ascorbate (with or without $\text{A}\beta$) provide just over 300 nM detectable H_2O_2 when the Amplex Red reagents are added at the end of the 1-h incubation period. This result shows that $\text{A}\beta$ neither prevents nor promotes H_2O_2 production by copper under these conditions when compared to copper in the presence of glycine as a carrier ligand, a result also seen by others. [12] In contrast, 8HQ inhibits H_2O_2 production, even when present at only a 0.25 equiv of Cu^{2+} . When 8HQ is present at a 2:1 ratio to Cu^{2+} , the amount of detectable H_2O_2 diminishes to one third that detected in

the absence of 8HQ. This result confirms that 8HQ coordinates Cu^{2+} in a manner that diminishes its ability to catalyze the formation of H_2O_2 from O_2 in the presence of reductant.

When QBP is added to the reaction mixture in place of 8HQ, similar results are obtained. As shown in Figure 6, samples that contain 200 μM QBP along with Cu^{2+} , ascorbate, and $\text{A}\beta$ result in detection of ~ 100 nM H_2O_2 , which is a third of the concentration obtained in the absence of chelator.

If the Amplex Red/HRP reagents are included at the beginning of the incubations, then up to 500 nM H_2O_2 is detected (not shown). These data suggest that H_2O_2 degrades during the incubation period, possibly via Fenton reaction or hydrolysis. This experiment also provides the maximum amount of H_2O_2 produced by the $\text{Cu}/\text{A}\beta$ /ascorbic acid system under these conditions. Given this number and the rate constant for the QBP-to-8HQ conversion, the 200 μM QBP sample in Figure 6 gives a calculated yield of 90 nM 8HQ. The results in Figure 6 are consistent with this prediction, as they indeed show that 200 μM QBP provides protection against H_2O_2 formation that is similar to that of 50–200 nM 8HQ.

A current hypothesis about Alzheimer's is that oxidative stress is an early event in disease progression and that copper may be a culprit in promoting further oxidative damage. The results presented here indicate that prochelator QBP can be activated under conditions that mimic early Alzheimer's pathology where copper, $\text{A}\beta$, and biological reductants exacerbate ROS formation. Importantly, the prochelator itself does not prevent or disaggregate metal-promoted $\text{A}\beta$ aggregates if they are not accompanied by elevated H_2O_2 . This feature may be beneficial as it may not be desirable to disaggregate stable plaques in the absence of ROS. Once activated to its unmasked form, however, the released 8HQ diminishes copper's ROS-forming reactivity, resolubilizes existing metal-associated aggregates, and inhibits further $\text{A}\beta$ aggregation. The H_2O_2 trigger incorporated into QBP provides just one level of specificity for targeting a chelating agent to a local environment with an elevated H_2O_2 concentration; it does not target the agent to amyloid-dense regions. Future work, therefore, will focus on incorporating amyloid-binding units[35,36] into the prochelator structure to create multifunctional agents directed to both the structure and reactivity of amyloid-beta.

Experimental Section

Experimental procedures, including synthesis, turbidity and hydrogen peroxide assays, peptide preparation and oxidation kinetic studies, are available in the Supporting Information. CCDC 743258 (QBP) contains the supplementary crystallographic data for this paper. These data can be obtained free of charge from The Cambridge Crystallographic Data Centre via www.ccdc.cam.ac.uk/data_request/cif.

Supplementary Material

Refer to Web version on PubMed Central for supplementary material.

Acknowledgments

KJF thanks the Sloan Foundation, the Camille and Henry Dreyfus Foundation, and the National Institutes of Health (grant GM084176) for supporting this work; MGD acknowledges a C.R. Hauser Fellowship from Duke University.

References

1. Hardy J, Selkoe DJ. *Science* 2002;297:353–356. [PubMed: 12130773]
2. Roychaudhuri R, Yang M, Hoshi MM, Teplow DB. *J Biol Chem* 2009;284:4749–4753. [PubMed: 18845536]

3. Bush AI. Trends Neurosci 2003;26:207–214. [PubMed: 12689772]
4. Gaggelli E, Kozlowski H, Valensin D, Valensin G. Chem Rev 2006;106:1995–2044. [PubMed: 16771441]
5. Treiber C, Simons A, Strauss M, Hafner M, Cappai R, Bayer TA, Multhaup G. J Biol Chem 2004;279:51958–51964. [PubMed: 15465814]
6. Zou K, Gong JS, Yanagisawa K, Michikawa M. J Neurosci 2002;22:4833–4841. [PubMed: 12077180]
7. Baruch-Suchodolsky R, Fischer B. Biochemistry 2009;48:4354–4370. [PubMed: 19320465]
8. Rauk A. Dalton Trans 2008:1273–1282. [PubMed: 18305836]
9. Huang X, Cuajungco MP, Atwood CS, Hartshorn MA, Tyndall JDA, Hanson GR, Stokes KC, Leopold M, Multhaup G, Goldstein LE, Scarpa RC, Saunders AJ, Lim J, Moir RD, Glabe C, Bowden EF, Masters CL, Fairlie DP, Tanzi RE, Bush AI. J Biol Chem 1999;274:37111–37116. [PubMed: 10601271]
10. Opazo C, Huang X, Cherny RA, Moir RD, Roher AE, White AR, Cappai R, Masters CL, Tanzi RE, Inestrosa NC, Bush AI. J Biol Chem 2002;277:40302–40308. [PubMed: 12192006]
11. Tabner BJ, El-Agnaf OMA, Turnbull S, German MJ, Paleologou KE, Hayashi Y, Cooper LJ, Fullwood NJ, Allsop D. J Biol Chem 2005;280:35789–35792. [PubMed: 16141213]
12. Nadal RC, Rigby SEJ, Viles JH. Biochemistry 2008;47:11653–11664. [PubMed: 18847222]
13. Guilloureau L, Combalbert S, Sourmia-Saquet A, Mazarguil H, Faller P. Chem BioChem 2007;8:1317–1325.
14. Castellani RJ, Honda K, Zhu XW, Cash AD, Nunomura A, Perry G, Smith MA. Age Res Rev 2004;3:319–326.
15. Smith DP, Smith DG, Curtain CC, Boas JF, Pilbrow JR, Ciccotosto GD, Lau TL, Tew DJ, Perez K, Wade JD, Bush AI, Drew SC, Separovic F, Masters CL, Cappai R, Barnham KJ. J Biol Chem 2006;281:15145–15154. [PubMed: 16595673]
16. Cuajungco MP, Goldstein LE, Nunomura A, Smith MA, Lim JT, Atwood CS, Huang X, Farrag YW, Perry G, Bush AI. J Biol Chem 2000;275:19439–19442. [PubMed: 10801774]
17. Cardoso SM, Rego AC, Pereira C, Oliveira CR. Neurotox Res 2005;7:273–281. [PubMed: 16179264]
18. Meloni G, Sonois V, Delaine T, Guilloureau L, Gillet A, Teissie J, Faller P, Vasak M. Nat Chem Biol 2008;4:366–372. [PubMed: 18454142]
19. Atwood CS, Obrenovich ME, Liu T, Chan H, Perry G, Smith MA, Martins RN. Brain Res Rev 2003;43:1–16. [PubMed: 14499458]
20. Bush AI. J Alzheimer's Dis 2008;15:223–240.
21. Adlard PA, Cherny RA, Finkelstein DI, Gautier E, Robb E, Cortes M, Volitakis I, Liu X, Smith JP, Perez K, Laughton K, Li QX, Charman SA, Nicolazzo JA, Wilkins S, Deleva K, Lynch T, Kok G, Ritchie CW, Tanzi RE, Cappai R, Masters CL, Barnham KJ, Bush AI. Neuron 2008;59:43–55. [PubMed: 18614028]
22. Ritchie CW, Bush AI, Mackinnon A, Macfarlane S, Mastwyk M, MacGregor L, Kiers L, Cherny R, Li QX, Tammer A, Carrington D, Mavros C, Volitakis I, Xilinas M, Ames D, Davis S, Beyreuther K, Tanzi RE, Masters CL. Arch Neurol 2003;60:1685–1691. [PubMed: 14676042]
23. Madsen E, Gitlin JD. Annu Rev Neurosci 2007;30:317–337. [PubMed: 17367269]
24. Benvenisti-Zarom L, Chen J, Regan RF. Neuropharmacol 2005;49:687–694.
25. Charkoudian LK, Dentchev T, Lukinova N, Wolkow N, Dunaief JL, Franz KJ. J Inorg Biochem 2008;102:2130–2135. [PubMed: 18835041]
26. Charkoudian LK, Pham DM, Franz KJ. J Am Chem Soc 2006;128:12424–12425. [PubMed: 16984186]
27. Charkoudian LK, Pham DM, Kwan A, Vangeloff A, Franz KJ. Dalton Trans 2007:5031–5042. [PubMed: 17992288]
28. Weir RJ, Fisher RS. Toxicol Appl Pharmacol 1972;23:351–364. [PubMed: 4673567]
29. Rezanka T, Sigler K. Phytochem 2008;69:585–606.
30. Scott LE, Orvig C. Chem Rev 2009;109:4885–4910. [PubMed: 19637926]
31. Mancino AM, Hindo SS, Kochi A, Lim MH. Inorg Chem 2009;48:9596–9598. [PubMed: 19817493]

32. Huang X, Atwood CS, Moir RD, Hartshorn MA, Vonsattel JP, Tanzi RE, Bush AI. *J Biol Chem* 1997;272:26464–26470. [PubMed: 9334223]
33. Storr T, Scott LE, Bowen ML, Green DE, Thompson KH, Schugar HJ, Orvig C. *Dalton Trans* 2009:3034–3043. [PubMed: 19352532]
34. Deraeve C, Boldron C, Maraval A, Mazarguil H, Gornitzka H, Vendier L, Pitié M, Meunier B. *Chem Eur J* 2008;14:682–696.
35. Dedeoglu A, Cormier K, Payton S, Tseitlin KA, Kremsky JN, Lai L, Li XH, Moir RD, Tanzi RE, Bush AI, Kowall NW, Rogers JT, Huang XD. *Exp Gerontol* 2004;39:1641–1649. [PubMed: 15582280]
36. Rodriguez-Rodriguez C, Sanchez de Groot N, Rimola A, Alvarez-Larena A, Lloveras V, Vidal-Gancedo J, Ventura S, Vendrell J, Sodupe M, Gonzalez-Duarte P. *J Am Chem Soc* 2009;131:1436–1451. [PubMed: 19133767]

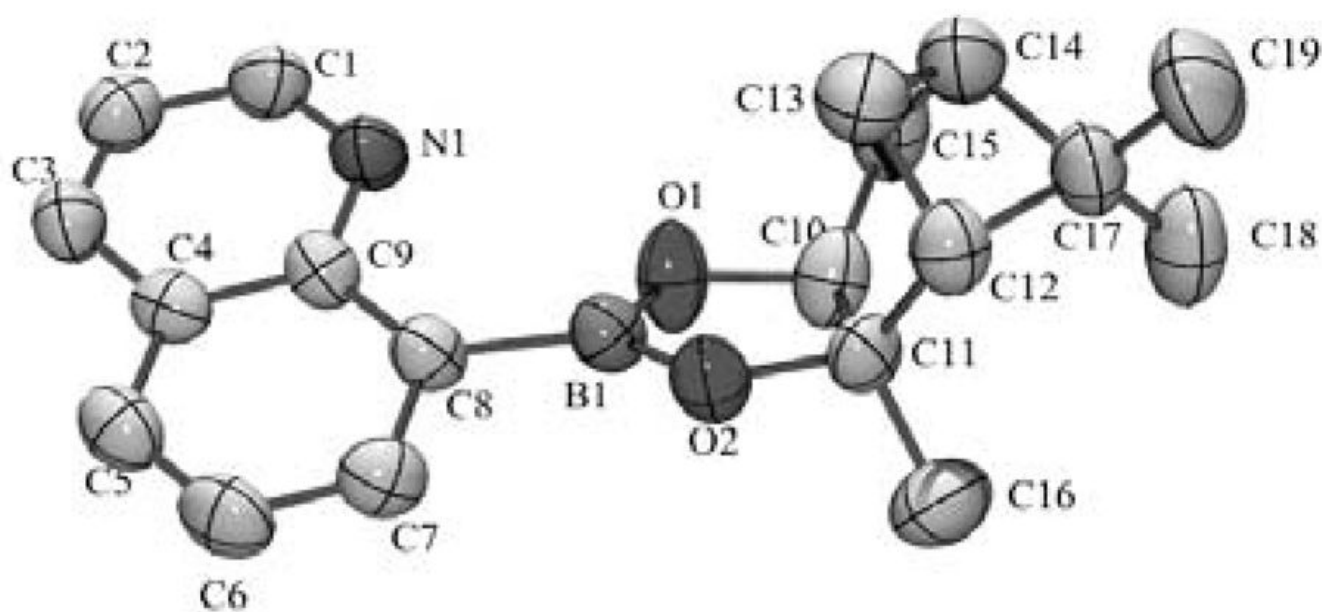


Figure 1.
Xray structure of QBP. Thermal ellipsoids are shown at 50% probability. Hydrogen atoms have been omitted for clarity.

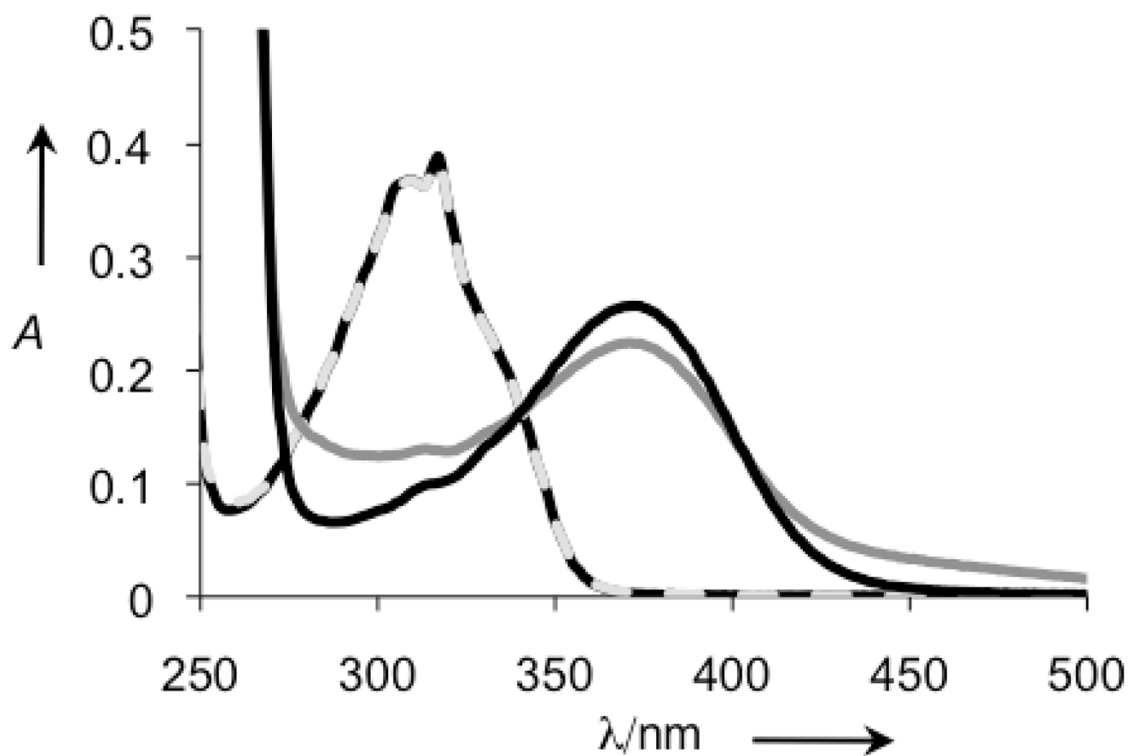


Figure 2. UV-vis spectra of 100 μM QBP in PBS pH 7.4 in the absence (---) and presence (— · —) of 50 μM $\text{Cu}(\text{Gly})_2$, and 60 min after treatment of the QBP/Cu sample with 4 mM H_2O_2 (—) The resulting spectrum is nearly identical to that of independently prepared $[\text{Cu}(\text{8HQ})_2]$ (—).

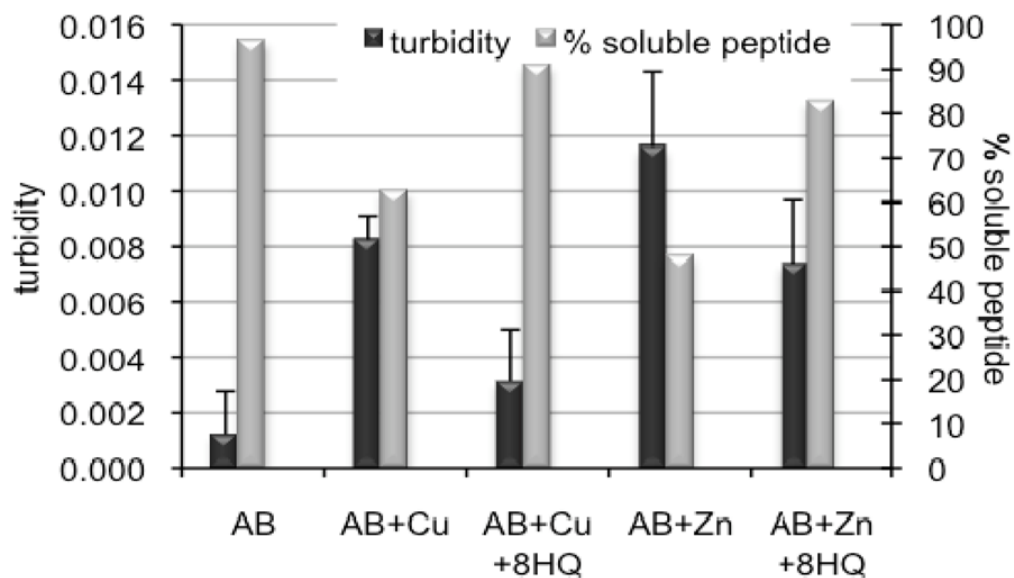


Figure 3.

Turbidity assay, as monitored by the difference in absorbance at 405 nm between the sample and its matched control that does not contain A β . Samples containing 10 μ M A β were incubated with 10 μ M Cu(Gly)₂ or ZnCl₂ in the presence or absence of 20 μ M 8HQ for 1 h at 37 °C. A₄₀₅ readings were taken 1 h after mixing (black, left-hand bars). The % soluble peptide remaining after 1 h was determined by a BCA protein concentration assay (gray, right-hand bars) on centrifuged samples.

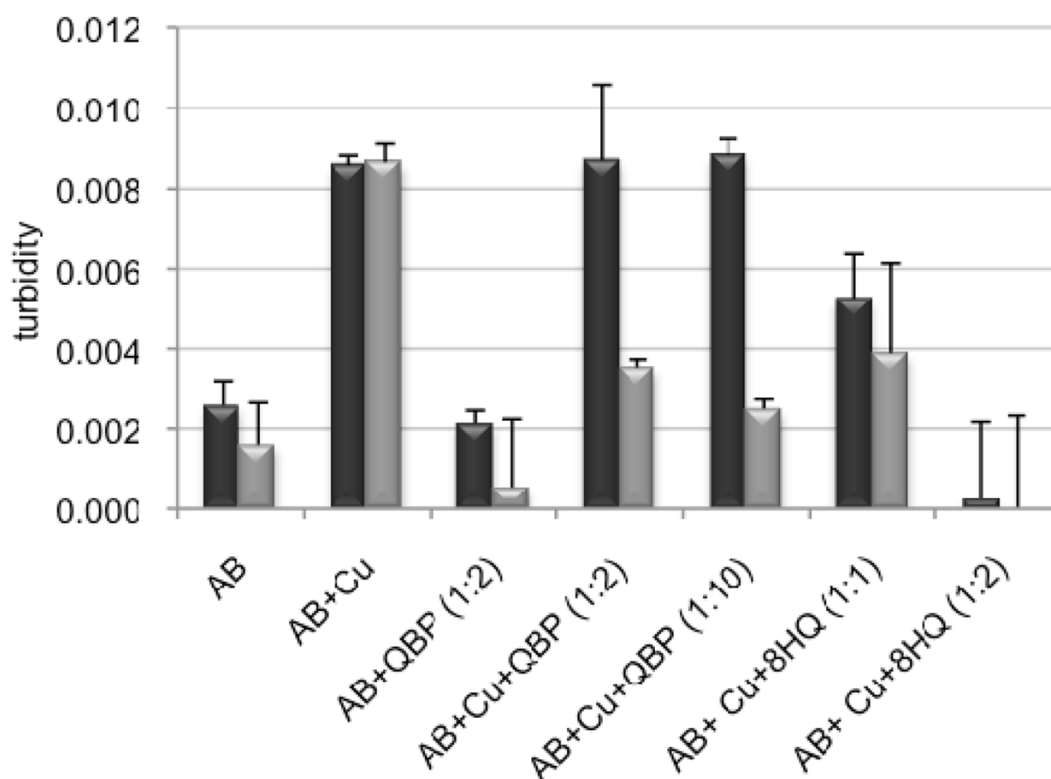


Figure 4.

Turbidity assay, as monitored by the difference in absorbance at 405 nm between the sample and its matched control that does not contain A β . Samples contain combinations of 10 μ M A β , 10 μ M Cu²⁺ (provided as Cu(Gly)₂), 20–100 μ M QBP, or 10–20 μ M 8HQ, as indicated. A₄₀₅ readings were taken 1 h after mixing (black bars), then again 30 min after addition of 1 mM H₂O₂ (gray bars).

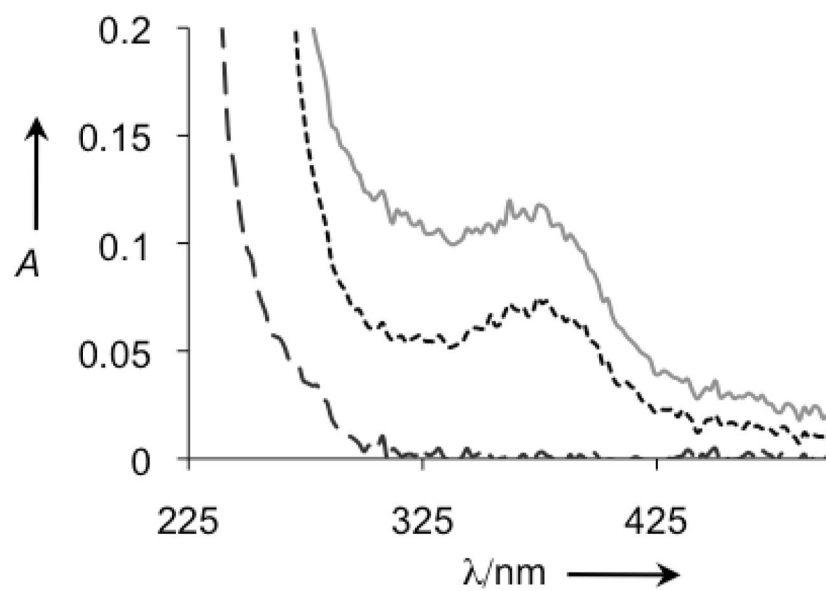
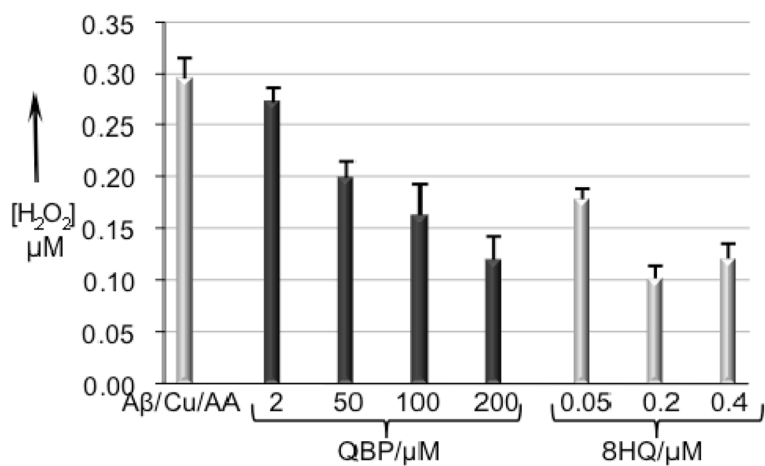
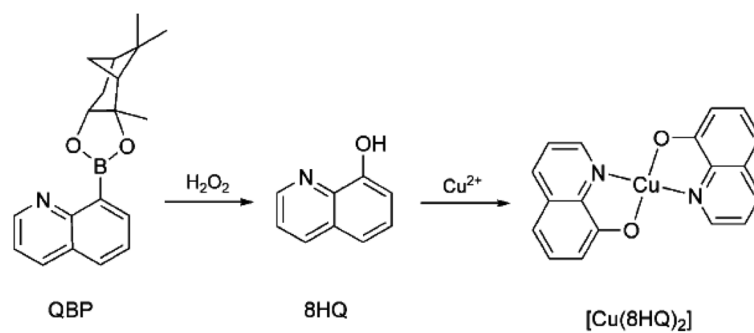


Figure 5. UV-vis analysis of H₂O₂-treated Aβ samples from Figure 4. — : Aβ+H₂O₂; - - - : Aβ+Cu+8HQ+H₂O₂; — : Aβ+Cu+QBP+H₂O₂.

**Figure 6.**

Hydrogen peroxide detection by the Amplex Red/HRP assay for samples containing various combinations of 200 nM A β , 200 nM Cu(Gly)₂, 10 μM ascorbic acid, 2–200 μM QBP, 200–400 nM 8HQ, in a total volume of 50 μL buffer (50 mM hepes, 150 mM NaCl). Samples were incubated at 37 °C for 1 h before 50 μL of Amplex Red/HRP reagent was added. Fluorescence readings were taken with λ_{ex} = 485 and λ_{em} = 590 nm.

**Scheme 1.**

Oxidation of QBP by H_2O_2 and subsequent binding of copper by 8-hydroxyquinoline (8HQ).